Velocity Relaxation of Fast Hydrogen Atoms by Collisions with Rare Gases, N_2, O_2, and N_2O

Seung Keun Shin, Tae Yeon Kang, and Hong Lae Kim*

Department of Chemistry, Kangwon National University, Chuncheon 200-701, Korea

Chan Ryang Park

Department of Chemistry, Kookmin University, Seoul 136-702, Korea

Received: September 21, 1999; In Final Form: December 7, 1999

Velocity relaxation of fast hydrogen atoms colliding with rare gas atoms, N_2, O_2, and N_2O molecules has been investigated by measuring Doppler broadened H atom spectra. The fast hydrogen atoms were generated by photodissociation of H_2S at 243.2 nm, and the H atom spectra were measured by two photon absorption laser induced Lyman-α fluorescence. The H atom spectra show an anisotropic velocity distribution with the anisotropy parameter, $\beta = -1.0 \pm 0.05$, without any colliding gases. Degradation of the anisotropy of the angular distribution was measured as a function of pressure of the colliding gases, He, Ar, Kr, N_2, O_2, and N_2O and the collision cross sections for velocity direction change were measured.

I. Introduction

Quenching energetic atoms by elastic and inelastic collisions with surrounding bath gases is one of the fundamental processes taking place in the upper atmosphere and in chemical reactors as well. The energetic atoms are often generated by photodissociation, photoelectron impact dissociation, dissociative recombination, and so forth. The collisions in some cases produce rovibrationally excited molecules that would undergo chemical reactions. Thus, detailed understanding of the collision processes is crucial to analyze subsequent physical and chemical processes.

The collisions of energetic atoms have been theoretically studied by numerically solving the Boltzmann equation for non-Maxwellian anisotropic velocity distribution.[1] The velocity distribution depends on both the direction and magnitude (speed) of the velocity. The eigenvalues of the collision operator depend on the mass ratio, $\gamma \equiv m_B/m_T$, where m_B and m_T are the masses of the bath gases and target atoms, respectively. When $\gamma \gg 1$, the distribution over angles is relaxed much more rapidly than the distribution over magnitudes, whereas the opposite is true for $\gamma \ll 1$. Experiments have been reported for each of the extremes and an intermediate case. Park et al. measured thermalization cross sections for fast hydrogen atoms colliding with rare gas atoms.[2] They found rapid relaxation of the angular part of the velocity distribution and slower relaxation of the radial part. Cline et al. found for the case of energetic I atoms that relaxation of the speed preceded relaxation of the angularly dependent part of the velocity distribution.[3] Matsumi et al. measured the rate of both relaxation processes for superthermal $O(^1D)$ atoms colliding with rare gas atoms and N_2 molecules.[4,5]

The collision cross sections of the hydrogen atom with rare gases were measured by crossed beam experiments at collision energies under 1.5 eV and interatomic potentials were deduced.[6,7] We report in this paper the collision cross sections for the fast hydrogen atoms produced by photodissociation of H_2S collided with rare gases and N_2, O_2, and N_2O molecules. We photolyzed the H_2S molecules with a nanosecond laser pulse and detected the H atoms by two-photon absorption and induced fluorescence within the same laser pulse. By using polarized laser light, we measured the Doppler profile of the H atom spectra showing anisotropic velocity distribution. Thus, we prepared an ensemble of the hydrogen atoms with an anisotropic velocity distribution and measured the degradation of the anisotropy by collisions with bath gases as a function of bath gas pressures. In this way, the cross sections for the direction changing collisions taking place in the early stage of the relaxation processes were measured.

II. Experiment

The experiment was performed in a flow cell with two arms in which baffles are placed to minimize scattered radiation. The cell was evacuated to a pressure of 10^{-3} Torr with a mechanical pump. The hydrogen atoms were generated by photodissociation of H_2S slowly flowing through the cell at a sample pressure of about 120 mTorr which was measured by a Baratron gauge.

The horizontally polarized 243.2 nm photolysis light was a frequency-doubled output of a dye laser (Lumonics HD-500) pumped by the second harmonic of a pulsed Nd:YAG laser (Lumonics YM-800). The temporal profile of the light pulse was measured with a fast photodiode (Hamamatsu) and found to be a Gaussian shape with fwhm of 7 ns (Figure 1). However, it is believed that the measured value is an upper bound because of the RC time of the detection electronics. The nominal fwhm value is supposed to be about 5 ns. The hydrogen atoms generated in the 1s state were then excited to the 2s state by subsequently absorbing two more photons of the same wavelength within the same light pulse and collisionally quenched to the 2p state followed by emission of Lyman-α fluorescence at 121.6 nm. The induced Lyman-α fluorescence was detected at a right angle to the laser beam by a solar blind photomultiplier tube (Hamamatsu R1259) through a Lyman-α filter. To maximize the signal-to-noise (S/N) ratio in the spectra, dry nitrogen was flowed between the PMT and the LiF viewing

* Corresponding author e-mail: hlkim@cc.kangwon.ac.kr.

10.1021/jp993385k CCC: $19.00
Published on Web 01/27/2000

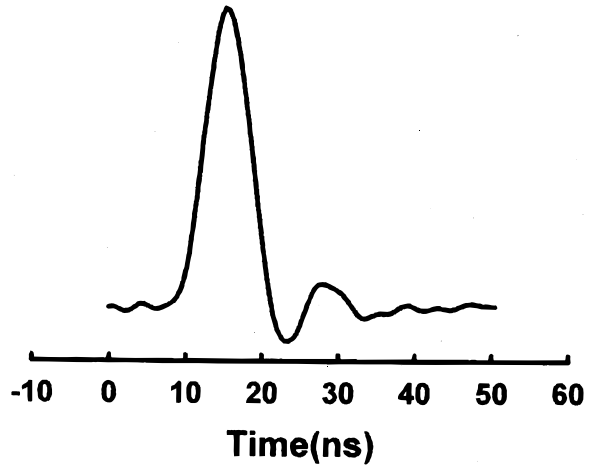

Figure 1. A temporal profile of the light pulse measured with a fast photodiode. The fwhm value is 7 ns.

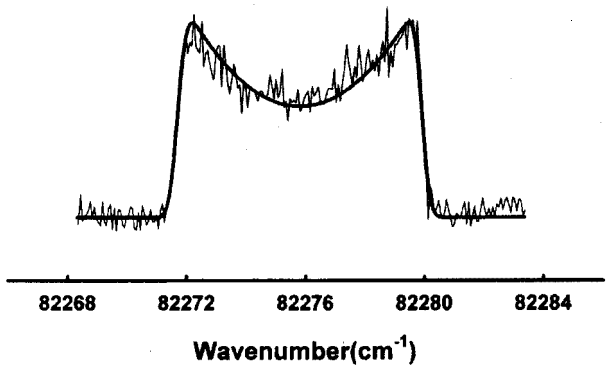

Figure 2. Doppler broadened spectrum of the H atom produced from photodissociation of H_2S at 243 nm. The solid line is the best fit to the observed spectrum by the equation in the text.

window. The line width of the laser is 0.06 cm^{-1} in the visible measured from rotationally resolved gaseous I_2 spectra at ambient temperature. The Doppler broadened laser induced fluorescence excitation spectra of H atoms were then measured with a gated integrator and a signal processor.

The maximum energy of the 243.2 nm light obtained from our system is about 3 mJ/pulse. Since this photodissociation and detection of H atoms requires at least three photons, the light was focused with a lens. To test power saturation and effect of the spot size at the focal point, the lenses with various focal lengths were used.

The Doppler broadened H atom spectra were measured in a static cell in the presence of various bath gases. The sample pressure of H_2S was fixed as 100 mTorr and the spectra were measured by adding He, Ar, Kr, N_2, O_2, or N_2O at different pressures up to about 30 Torr. The gases were purchased from Aldrich, Spectra Gases, and local companies with stated purities higher than 99% and used without further purification.

III. Results

A typical Doppler broadened H atom spectrum is presented in Figure 2. Since the photolysis and probe have been achieved by the same light pulse, the polarization direction of the photolysis light, ϵ_d, is perpendicular to the propagation direction of the probe light, k_p, that is, $\epsilon_d \perp k_p$. The angular distribution of the photofragments is described by the equation[8]

$$I(\theta) = \frac{1}{4\pi}[1 + \beta P_2(\cos\theta_{\epsilon,v})]$$

assuming instantaneous dissociation upon absorption of the light. In the above equation, $\theta_{\epsilon,v}$ is the angle between ϵ_d and recoil direction, v, of the photofragment, P_2 is the second-order Legendre polynomial, and β is the anisotropy parameter which reveals the angular distribution of the fragments. The anisotropy parameter β has the limiting value of 2 for the parallel transition (the transition dipole moment aligned parallel to the recoil direction), while for the perpendicular transition, it is -1. According to the addition theorem for Legendre polynomials, the above equation then becomes

$$I(\theta) = \frac{1}{4\pi}[1 + \beta P_2(\cos\theta_{\epsilon,z})P_2(\cos\theta_{v,z})]$$

where $\theta_{\epsilon,z}$ and $\theta_{v,z}$ are the angles of ϵ_d and v to the probe direction z. Since the experimental geometry of this study is $\epsilon_d \perp z$ and the Doppler shift of the absorption frequency, ν compared to ν_0 of the atom at rest is given by

$$\nu = \nu_0\left(1 + \frac{v}{c}\cos\theta_{v,z}\right)$$

the Doppler broadened profile of the spectra becomes

$$I(\nu) = \frac{1}{4\pi}\left[1 - \frac{1}{4}\beta\left\{3\left(\frac{\nu - \nu_0}{\nu_0}\right)^2\left(\frac{c}{v}\right)^2 - 1\right\}\right]$$

The observed H atom spectra were fitted well by the above equation with a speed of 14 800 m/s and $\beta = -1.0 \pm 0.05$, implying that the transition dipole moment is aligned perpendicular to the molecular plane. From the speed of the H atoms, the fraction of the available energy (the photon energy minus the bond dissociation energy) released as translation is calculated to be 0.96.

As mentioned in the Experimental Section, the spectra were measured under various experimental conditions in order to test the saturation and the effect of the spot size at the focal point. We have tested the lenses of $f = 15$, 50, and 100 cm with the laser power from 300 μJ/pulse to 3 mJ/pulse. At very high light densities such as $f = 15$ cm and 2 mJ/pulse, the spectra showed saturation. Besides, since the generated H atom is moving fast, 14 800 m/s, it can escape from the viewing zone during the probing period 5−7 ns when the light beam is tightly focused. Thus, the spectra were measured with the laser power kept as low as possible and with the lens, $f = 100$ cm which has the diameter of the spot size of at least >300 μm at the focal point. The log−log plot of the measured signal intensities vs the laser power shows a straight line with the slope of 3.3 ± 0.2 (Figure 3). This slope is consistent with a one-photon dissociation process followed by a two-photon probe process.

In Figure 4, the Doppler broadened spectra of the H atoms collided by Ar gas at different pressures are shown. The spectra show an apparent increase of the anisotropy parameter, β from -1 under no collisions to 0 as the Ar pressure increases. From the above equation, the spectra of the rectangular shape should be expected when the angular distribution of the H atoms becomes isotropic ($\beta = 0$). The direction changing collision is so effective, that is, the cross section for the direction changing collision is so large, that the evolution of the Doppler broadened line shape may be very sensitive to the small number of average collisions. In the meantime, however, transfer of the translational energy seems to be ineffective, which is reflected by almost no change in the line width of the profiles. The apparent βs as a function of the pressure of various colliding gases were measured and plotted in Figure 5. As seen in the figure, the

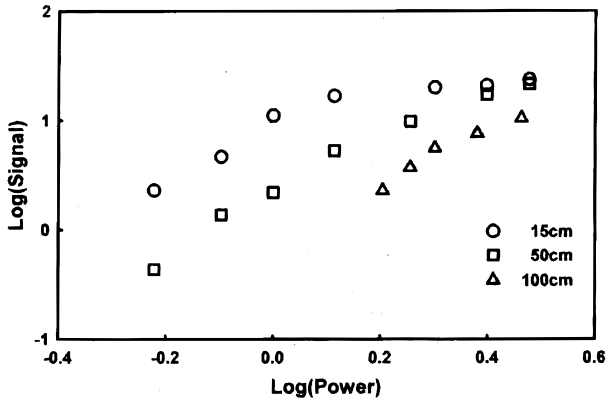

Figure 3. Log-log plot of the measured signal intensities vs the laser powers. Symbols indicated are from lenses of different focal lengths. The plots show linear slopes of 3.3 ± 0.2 with saturation at high powers.

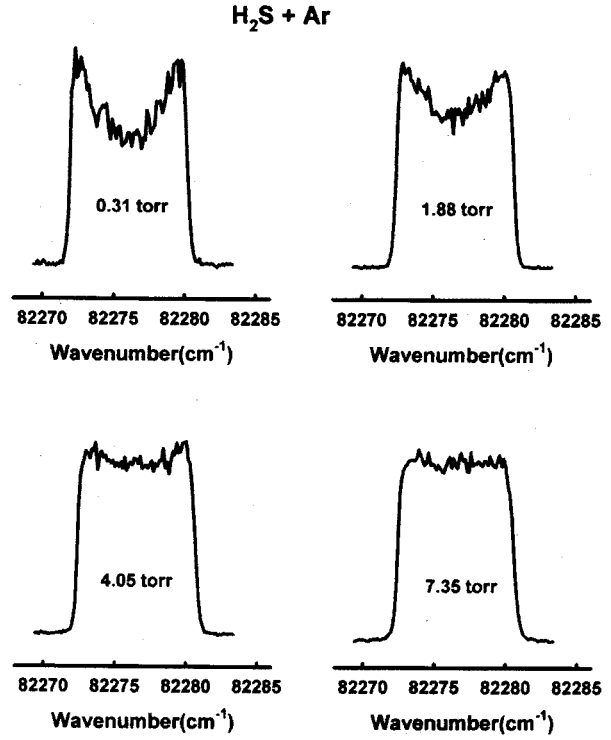

Figure 4. Doppler broadened H atom spectra at different Ar bath gas pressures.

cross sections are expected to be larger for the atoms or molecules of larger masses.

IV. Discussions

A. Photodissociation Dynamics of H_2S. Studies of photodissociation dynamics of H_2S excited within the first continuum have been reported by many authors. The absorption starts from around 250 nm and peaks about 200 nm with diffuse bands at shorter wavelengths superimposed by a broad continuum.[9] In the previous studies, angular and internal energy distributions of the SH fragments at various photolysis wavelengths within the first continuum were measured.[10−14] The dissociation dynamics was also studied by measuring emission spectra of dissociating H_2S molecules.[15,16] All of these measurements suggest that the transition is induced by $b_1 \rightarrow a_1$ electron promotion in the C_{2v} symmetry. Electronic structure calculations predict that the excited states responsible for the transition are mainly the $^1B_1$ and $^1A_2$ states.[17−19] The H_2S molecule is initially

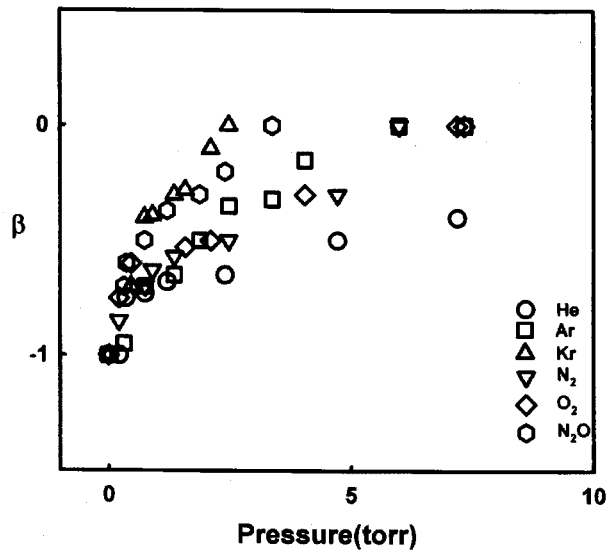

Figure 5. Measured average anisotropy parameter βs as a function of various bath gas pressures.

excited to the $^1B_1$ state that is bound along the symmetric stretching vibrational coordinate at the Franck−Condon region. The $^1B_1$ state is crossed by the repulsive $^1A_2$ state near the bottom of the $^1B_1$ potential energy surface forming a conical intersection. Recent measurements of the emission spectra of H_2S excited at 199−203 nm clearly show an evidence of the conical intersection near 200 nm.[16] Upon excitation of H_2S near and above the conical intersection, the excited molecule initially feels the force along the symmetric stretching vibrational coordinate. As the dissociating molecule samples the conical intersection, an influence by the $^1A_2$ state leads the molecule to the exit channel repulsive along the asymmetric stretching vibrational coordinate. In the adiabatic picture, however, the diabatic $^1B_1$ and $^1A_2$ states are correlated to the two $^1A''$ adiabatic surfaces along the asymmetric stretching vibrational coordinate in the C_s symmetry.[13] The $1^1A''$ state is purely repulsive and the $2^1A''$ state at higher energy is bound, both of which are all dipole allowed from the ground electronic state. The absorption is to both the repulsive $1^1A''$ state and the bound $2^1A''$ state leading to the structured absorption at the shorter wavelength side of the spectrum. The measured anisotropy parameter ($\beta = -1.0 \pm 0.05$) reveals that the transition at 243 nm is purely perpendicular, that is, the transition dipole moment lies perpendicular to the molecular plane. The fact that the fraction of the available energy distributed to the translational energy of the fragment is 0.96 with little vibrational excitation of SH is in good agreement with the previous results. The photodissociation of H_2S at 243 nm is prompt, at least the lifetime of the excited molecule is shorter than a rotational period. The two diabatic excited states, $^1B_1$ and $^1A_2$ are strongly coupled and are correlated to the adiabatic A″ surfaces along the asymmetric stretching vibrational coordinate. At 243 nm, the longer wavelength side of the first continuum and with energy below the conical intersection, the vertical transition from the ground state directly accesses the repulsive part of the $1^1A''$ adiabatic surface and the dissociation takes place along this potential surface.

B. Collision Cross Sections of H Atoms. The velocity distribution for atoms photodissociated from molecules with linearly polarized light can be written rigorously as

$$f(\vec{v},t) = f_0(\vec{v},t) + \beta f_{\text{coll}}(t) f_2(\vec{v},t) P_2(\cos\theta)$$

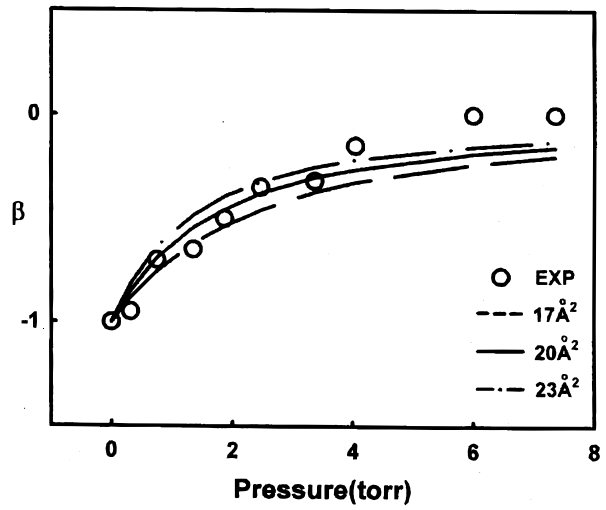

Figure 6. A typical fit of the observed βs as a function of the Ar bath gas pressures in order to obtain collision cross sections. The best fit is obtained for the experimental values at low pressures.

where β is the anisotropy parameter of the fragments. In a general case, $f_{coll}(t)$ would be absorbed in $f_2(\vec{v},t)$. In the present case, however, the specific assumption is made that the potential of interaction is that of two hard spheres. The experimental results will be shown to support this assumption. Relaxation of the anisotropy is shown by change in the shape of the Doppler broadened line as in Figure 4, while relaxation of the speed distribution is shown by reduction of the line width.[2] A single hard sphere collision results in an isotropic velocity distribution. Thus, at any given time, the atoms which have undergone no collisions preserve their initial anisotropic distribution. Let f_{coll} be the fraction of atoms which have undergone no collision. Then, the apparent measured β is given by

$$\beta = \beta(0) f_{coll}$$

where $\beta(0)$ is the anisotropy parameter of the H atoms without the bath gases, that is, -1 in the present experiment, and f_{coll} is the fraction of the H atoms experiencing no collisions. Because the collision takes place before the probing two photons are absorbed by the H atoms and the whole LIF signal is produced within the single laser pulse, f_{coll} is given by assuming the first-order rate process

$$f_{coll} = \frac{\int_0^t \int_0^\infty I(t) I^2(t') e^{-N v \sigma (t-t')} dt dt'}{\int_0^t \int_0^\infty I(t) I^2(t') dt dt'}$$

where $I(t)$ is the temporal pulse shape of the light, N is the number density of the bath molecules, v is the relative speed of the H atoms and bath gas molecules, and σ is the collision cross section. In this expression, the fraction is normalized to the total number of the H atoms produced. The apparent anisotropy parameter has been calculated as a function of the bath gas pressure with the H atom speed of 14 800 m/s and thermal speed of the bath molecules and fitted to the experimentally observed βs by varying the collision cross sections. A typical fit is presented in Figure 6 for the Ar case. From the best fit, the collision cross sections have been found and listed in Table 1.

As can be seen in Figure 1, there is a ringing in the temporal profile of the light pulse because of the detector noise. To see this ringing effect on the measured cross section, the fitting of the data was repeated with the smooth Gaussian function with 7 ns fwhm for $I(t)$ and compared the cross section values. The obtained values are not significantly different from those measured from the experimental temporal profiles, mainly within the error bounds. The fitting seems to be deviated from the experiments at high pressures as seen in Figure 6. The deviation mainly originates from the single speed assumption of the H atoms. Since the mass of the colliding gases is not infinite, energy transfer takes place by collisions. As the pressure increases, the H atoms after the collision have different speeds and the distribution of speed affects the experimentally observed Doppler profiles, which results in more rapid convergence of the experimentally measured anisotropy parameters to zero. Thus, the cross sections were obtained from the best fit at low pressures. In addition, in this fitting, the hard sphere collision and the first-order rate process is assumed. The deviation of the fit at high pressures might come from some small angle scattering collisions with larger cross sections due to short-range potential interactions. Contribution of these collisions to the anisotropy may be calculated if these realistic potentials would be known.

TABLE 1: Measured Collision Cross Sections (Å²) of the Fast H Atoms Colliding with Various Atoms and Molecules

	this work	thermalization
He	7 ± 2	10 ± 2^a
Ar	20 ± 3	9 ± 2^a
Kr	60 ± 5	12 ± 2^a
N_2	14 ± 2	
O_2	21 ± 2	
N_2O	32 ± 3	

[a] Reference 2.

The cross sections for direction changing collisions or disalignment cross sections depend on the masses of the colliding partners. When the fast H atom strikes a bath molecule or atom with infinite mass, in this case the atom could never lose kinetic energy but its velocity correlation would be zero. The cross sections measured in this work for collisions relaxing β to zero are larger than those reported by Park et al. for speed reducing collisions, implying that the direction changing collisions dominate energy transfer collisions as expected since the lightest H atom collides with the heavier gases.

Acknowledgment. This work has been financially supported by Korea Research Foundation. The authors thank Prof. Richard Bersohn for his helpful discussions on this manuscript.

References and Notes

(1) Shizgal, B.; Blackmore, R. *Chem. Phys.* **1983**, *77*, 417.
(2) Park, J.; Shafer, N.; Bersohn, R. *J. Chem. Phys.* **1989**, *91*, 7861.
(3) Cline, J. I.; Taatjes, C. A.; Leone, S. R. *J. Chem. Phys.* **1990**, *93*, 6543.
(4) Matsumi, Y.; Shamsuddin, S. A.; Sato, Y.; Kawasaki, M. *J. Chem. Phys.* **1994**, *101*, 9610.
(5) Balakrishnan, N.; Kharchenko, V.; Dalgarno, A. *J. Phys. Chem.* **1999**, *103*, 3999.
(6) Bickes, R. W., Jr.; Lantzsch, B.; Toennies, J. P.; Walaschewski, K. *Faraday Discuss. Chem. Soc.* **1973**, *55*, 167.
(7) Toennies, J. P.; Welz, W.; Wolf, G. *J. Chem. Phys.* **1979**, *71*, 614.
(8) Hall, G. E.; Houston, P. L. *Annu. Rev. Phys. Chem.* **1989**, *375*, 40.
(9) Lee, L. C.; Wang, X.; Suto, M. *J. Chem. Phys.* **1987**, *86*, 4353.
(10) Hawkins, W. G.; Houston, P. L. *J. Chem. Phys.* **1980**, *73*, 297.
(11) van Veen, G. N.; Mohamed, K. A.; Baller, T.; de Vries, A. E. *Chem. Phys.* **1983**, *74*, 261.
(12) Xu, Z.; Koplitz, B.; Wittig, C. *J. Chem. Phys.* **1987**, *87*, 1062.
(13) Xie, X.; Schneider, L.; Wallmeier, H.; Boettner, R.; Welge, K. H.; Ashfold, M. N. R. *J. Chem. Phys.* **1990**, *92*, 1068.

(14) Continetti, R. E.; Balko, B. A.; Lee, Y. T. *Chem. Phys. Lett*. **1991**, *182*, 400.

(15) Person, M. D.; Lao, K. Q.; Eckholm, B. J.; Butler, L. J. *J. Chem. Phys*. **1989**, *91*, 812.

(16) Browning, P. W.; Jensen, E.; Waschewski, G. C. G.; Tate, M. R.; Butler, L. J. *J. Chem. Phys.* **1994**, *101*, 5652.

(17) Weide, K.; Staemmler, V.; Schinke, R. *J. Chem. Phys*. **1990**, *93*, 861.

(18) Kulander, K. C. *Chem. Phys. Lett*. **1984**, *103*, 373.

(19) Dixon, R. N.; Marston, C. C.; Balint-Kurti, G. G. *J. Chem. Phys*. **1990**, *93*, 6520.